WATER RESOURCES RESEARCH, VOL. 34, NO. 11, PAGES 2837–2842, NOVEMBER 1998

Dual-energy synchrotron X ray measurements of rapid soil density and water content changes in swelling soils during infiltration

Patricia Garnier,[1] Rafael Angulo-Jaramillo,[2] David A. DiCarlo,[3] Tim W. J. Bauters,[1] Christophe J. G. Darnault,[1] Tammo S. Steenhuis,[1] J.-Yves Parlange,[1] and Philippe Baveye[4]

Abstract. Understanding soil swelling is hampered by the difficulty of simultaneously measuring water content and bulk density. A number of studies have used dual-energy gamma rays to investigate soil swelling. The long counting time of this technique makes it impracticable for studying the rapid changes in moisture content and soil swelling shortly after infiltration is initiated. In this paper, we use the dual-energy synchrotron X ray to measure, for the first time, the water content and bulk density changes during the fast, initial phase of the swelling process. Ponded infiltration experiments were performed with two soils: a bentonite-sand mixture and a vertisol. Swelling curves and hydraulic diffusivity were determined. Deformation was very rapid immediately after water application and then became progressively slower. The hydraulic diffusivity decreased with time, which can partially explain the very rapid decrease in infiltration rates observed in the field.

1. Introduction

The understanding of transport processes in swelling soils and materials is hampered by the difficulty of accurately measuring both the water content and the dry bulk density during the swelling process. Dual-energy gamma rays [*Nofziger and Swartzendruber*, 1974; *Angulo-Jaramillo*, 1989; *Barataud et al*., 1996; *Garnier et al*., 1997a] that are currently being used have a relatively low energy intensity and counting times that are too long for the characterization of the rapid swelling and decreasing infiltration rates shortly after the start of the rain [*Favre et al*., 1997].

Compared with conventional gamma rays, synchrotron X rays have a high intensity and brightness [*Batterman and Ashcroft*, 1979] and can make measurements up to 200 times faster with the same accuracy [*Angulo-Jaramillo*, 1989; *DiCarlo et al*., 1997]. Several studies have used single-energy synchrotron X rays: *Liu et al*. [1993] and *DiCarlo et al*. [1997] made rapid measurements of fluid contents for fingered flow in oil-water systems. *Charlie et al*. [1997] studied deformation of a saturated clay soil by consolidation using single-energy synchrotron X rays.

Dual-energy synchrotron X rays can measure two properties of the porous medium simultaneously. *DiCarlo et al*. [1997] simultaneously measured the oil and water contents of unstable fingered flow in oil-water-air systems. In this paper, we will use dual-energy synchrotron X rays to characterize, for the first time, the bulk density and the moisture content for two soils during the initial, fast phase of the swelling. These measurements are then used to derive the hydrological properties of the two soils.

[1]Department of Agricultural and Biological Engineering, Cornell University, Ithaca, New York.
[2]Laboratoire d'étude des Transferts en Hydrologie et Environnement, CNRS, INPG, ORSTOM, UJF, Grenoble, France.
[3]Department of Petroleum Engineering, Stanford University, Stanford, California.
[4]Laboratory of Environmental Geophysics, Cornell University, Ithaca, New York.

Paper number 98WR02367.
0043-1397/98/98WR-02367$09.00

2. Materials and Methods

2.1. Determination of Dry Bulk Density and Volumetric Water Content

The attenuation of radiation is linearly related to the amount of material within its path. In the case of a water-soil system, the attenuation A is [e.g., *DiCarlo et al*., 1997]

$$A = U_S\theta_s x - U_W\theta_W x + A_0 \tag{1}$$

where the subscripts S and W denote the solid and water phases, respectively, U is the attenuation constant, θ is the volumetric content, x is the thickness of the column, and A_0 is the attenuation due to the column walls and air between the detectors.

To study the movement of solid particles and water, two independent measurements are needed. They can be obtained from (1) by the attenuation measurements of radiation with two different energies: the high-energy attenuation A_H and the low-energy attenuation A_L. The volumetric solid and water contents can then be determined as [*DiCarlo et al*., 1997]

$$\theta_S = \frac{U_{WH}(A_L - A_{L0}) - U_{WL}(A_H - A_{H0})}{(U_{WL}U_{SH} - U_{WH}U_{SL})x} \tag{2a}$$

$$\theta_W = \frac{U_{SL}(A_H - A_{H0}) - U_{SH}(A_L - A_{L0})}{(U_{WL}U_{SH} - U_{WH}U_{SL})x} \tag{2b}$$

where the subscripts H and L denote the high and low energies, respectively.

The variance of the volumetric contents can be calculated following the technique described by *Oostrom et al*. [1995] and *DiCarlo et al*. [1997]:

Table 1. Measured Attenuation Constants of the Water, Bentonite-Sand Mixture, and Vertisol

Phase	Attenuation Coefficients, cm^{-1}	
	35-keV U_L	70-keV U_H
Water	0.115	0.186
Bentonite and sand	0.305	1.190
Vertisol	0.378	1.644

$$\text{Var}\,(\theta_W) = \frac{1}{t}\left(\frac{U_{SH}^2}{R_L} + \frac{U_{SL}^2}{R_H}\right)\left(\frac{1}{(U_{WL}U_{SH} - U_{WH}U_{SL})x}\right)^2 \quad (3a)$$

$$\text{Var}\,(\theta_S) = \frac{1}{t}\left(\frac{U_{WH}^2}{R_L} + \frac{U_{WL}^2}{R_H}\right)\left(\frac{1}{(U_{WL}U_{SH} - U_{WH}U_{SL})x}\right)^2 \quad (3b)$$

where R_L and R_H are the photon intensities incident on the detectors (photons per second) and t is the counting time.

2.2. Experimental Setup

A series of infiltration experiments was carried out in a 4 cm by 4 cm rectangular plexiglass chamber with two swelling materials: a mixture of fine sand and 8% (by weight) bentonite and a vertisol from Podor in the Senegal River Valley. The dry bentonite-sand mixture was wetted with distilled water until it reached a water content of 3.7% by weight. It was packed layer by layer (of ~1 cm) into the plexiglass column to a height of 3.6 cm, at a mean dry bulk density of 1.54 kg cm^{-3}, resulting in a mean volumetric water content of 0.057 cm^3 cm^{-3}. The soil layers were packed by tamping the soil 20 times. The vertisol was the same as that used by *Garnier et al*. [1997b] and was composed of 10% sand, 24% silt, and 66% clay. The clay fraction consisted of 60% smectite, 30% kaolinite, 5% illite, and 5% chlorite. The soil was sieved through a 200-μm screen and packed in the column to a height of 6.1 cm. The mean dry bulk density was 1.45 kg cm^{-3}.

After packing, the column was transported to the synchrotron facility and mounted on a movable platform that had a horizontal and vertical range of 25 and 50 cm, respectively, and a position repeatability of 0.1 mm. Measurements of bulk density and water content were monitored at 1-mm intervals by measuring the attenuation of the X rays. In 5 s, 5 cm of distilled water was ponded on the soil using a peristaltic pump. The experiments were continued for a duration of 300 min for the bentonite-sand mixture and 500 min for the vertisol.

2.3. X Ray Detection

The low and high energies used in the experiments were 35 and 70 kv, respectively. The flux of photons incident on the detectors was ~12,000 photons per second for the low-energy beam and 22,000 photons per second for the high-energy beam (R_L and R_H, respectively, in (3a) and (3b)). The counting time was 1 s for the bentonite-sand mixture and 5 s for the vertisol. Attenuation constants for the two soils and water were obtained by measuring the X ray attenuation of different widths of each material. Attenuation constants are the slopes of the curve of the attenuation (A in our notation) versus $\theta_s x$ (to calculate the attenuation constant of solid) or $\theta_w x$ (to calculate the attenuation constant of water) using (1). Table 1 gives the attenuation constants for both materials and both energies. Attenuations of the empty columns (A_{H0} and A_{L0} in (2a) and (2b)) were determined before each experiment.

2.4. Determination of the Hydraulic Properties

The swelling curve and hydraulic diffusivity can be calculated from the profiles of solid particle content θ_S and volumetric water content θ_W at different times. The swelling curve $e(\vartheta)$ relates the moisture ratio ϑ (water volume/solid volume) to the void ratio e (void volume/solid volume), and it can be obtained from the dry bulk density ρ_d (mass of solid particles per total volume of soil) and the volumetric water content θ_W as

$$\vartheta = \theta_w \frac{\rho_S}{\rho_d} \quad (4a)$$

$$e = \frac{\rho_S}{\rho_d} - 1 \quad (4b)$$

where

$$\rho_d = \rho_S \theta_S \quad (5)$$

where ρ_S is the specific density of the solid soil particles.

In swelling soils the water flux $q_{W/S}$ is often expressed in a coordinate system that is associated with the solid phase (the Lagrangian coordinate frame) [*Smiles and Rosenthal*, 1968; *Philip*, 1969; *Garnier et al*., 1997a; *Gérard-Marchant et al*., 1997]. It can be calculated from the knowledge of the water and solid fluxes, $q_{W/0}$ and $q_{S/0}$, respectively, expressed in a fixed coordinate system (the Eulerian coordinate frame) from the following equation [*Angulo-Jaramillo*, 1989]:

$$q_{W/S} = q_{W/0} - (\theta_W/\theta_S) q_{S/0} \quad (6)$$

Neglecting gravity, the fluxes $q_{S/0}$, $q_{W/0}$, and $q_{W/S}$ are given from Darcy's law by the following equations:

$$q_{S/0} = -D_{S/0}(\partial \theta_S/\partial z) \quad (7a)$$

$$q_{W/0} = -D_{W/0}(\partial \theta_W/\partial z) \quad (7b)$$

$$q_{W/S} = -D_{W/S}(\partial \theta_W/\partial z) \quad (7c)$$

where $D_{S/0}$ and $D_{W/0}$ are the apparent diffusivities of solid particles and water, respectively, in the Eulerian coordinate system and $D_{W/S}$ is the diffusivity of water in the Lagrangian coordinate system.

Substituting (7a)–(7c) into (6), one obtains the hydraulic diffusivity relative to the solid phase, $D_{W/S}$, as

$$D_{W/S} = D_{W/0} - (\theta_W/\theta_S)(d\theta_S/d\theta_W) D_{S/0} \quad (8)$$

Thus the hydraulic diffusivity in the Lagrangian coordinate system is obtained by adding a term to the hydraulic diffusivity in the Eulerian system, $D_{W/0}$, that depends on both the apparent solid diffusivity $D_{S/0}$ and the relationship $\theta_W(\theta_S)$ that is obtained from the swelling curve $e(\vartheta)$. As expected for rigid soils, this second term vanishes.

The apparent diffusivities $D_{W/0}$ and $D_{S/0}$ were calculated using the instantaneous profile method [*Watson*, 1966] according to (7a) and (7b) from the experimental volumetric content profiles. The fluxes of solid particles, $q_{S/0}$, and water, $q_{W/0}$, are evaluated on the basis of the water content and solid particle content profiles at time t and $t + \Delta t$ (Δt is a small time increment) using the following equations [*Vachaud et al*., 1978]:

$$q_{S/0} = \frac{\int_L^z \theta_S(\bar{z}, t)\, d\bar{z} - \int_L^z \theta_S(\bar{z}, t + \Delta t)\, d\bar{z}}{\Delta t} \quad (9a)$$

$$q_{W/0} = \frac{\int_L^z \theta_W(\bar{z}, t)\, d\bar{z} - \int_L^z \theta_S(\bar{z}, t + \Delta t)\, d\bar{z}}{\Delta t} \quad (9b)$$

where z is an arbitrary height and L is the height where the water and solid fluxes are equal to zero. The hydraulic diffusivity relative to the solid phase at a given time (equation (8)) was then calculated only from the knowledge of the experimental profiles θ_S and θ_W at that time.

3. Results and Discussion

3.1. Dry Bulk Density and Volumetric Water Content Profiles

The standard deviations of the solid particle content and the water content are calculated from the variances of (3a) and (3b) with the parameters given in section 2.3. For counting times of 5 s or less the standard deviations of the dry bulk density (related to the solid particle content with (5)) are 0.007 and 0.003 g cm^{-3} for the bentonite-sand mixture and vertisol, respectively. The values compare well with those obtained by *Angulo-Jaramillo* [1989] (0.01–0.03 g cm^{-3}) for the dual gamma ray system for counting times of 200 s. The volumetric water content standard deviations are 0.03 and 0.02 cm cm^{-3} for the bentonite-sand mixture and vertisol, respectively, for the synchrotron X ray, which is of the same order as the dual gamma ray measurements (0.01–0.04 cm cm^{-3}). The synchrotron X ray values of the bentonite-sand mixture are higher than those of the vertisol, owing to the longer counting time for the vertisol than for the bentonite-sand mixture. Moreover, bulk density measurements are more precise than the volumetric water content.

In both soils the initial dry bulk density was less for the first centimeter of the sample (Figures 1a and 2a). Increase with depth of the dry bulk density was also observed in the field [*Talsma and van der Lelij*, 1976] on cracked swelling soils.

For the bentonite-sand mixture (Figures 1a and 1b) the infiltration was very fast at the beginning of the experiment. After 2.6 min the infiltration front was almost 2 cm below the initial surface of the sample, and the soil heave was 0.4 cm. Infiltration decreased sharply after 14.9 min. Then the profiles changed very little. The profile at 278 min was close to the one at 14.9 min.

The total soil heave for the vertisol, 0.6 cm (Figures 2a and 2b), was less than that for the bentonite-sand mixture (1.4 cm). Both profiles show that the first top-centimeter of the soil behaves differently than the lower parts. The saturated volumetric water content of the first centimeter of the soil was 0.63 cm^3 cm^{-3}, whereas it was around 0.35 cm^3 cm^{-3} for the lower part, which can be explained by both the lower initial dry bulk density of the first centimeter and the dispersion of the surface clays. Indeed, we observed that the water just above the soil surface was cloudy owing to the presence of soil particles.

The changes in the dry bulk density of the vertisol were less important (except for the first centimeter) than those in the bentonite-sand mixture. Also, the infiltration front of the vertisol has a double-S shape that is more abrupt than that in the bentonite-sand mixture.

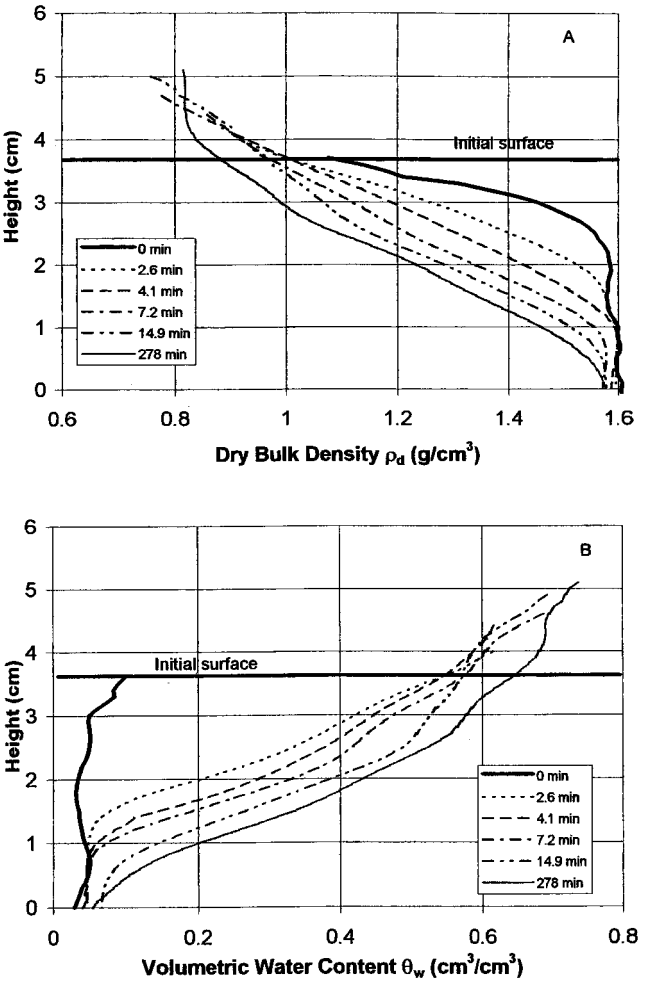

Figure 1. Observed profiles of (a) dry bulk density and (b) volumetric water content in the bentonite-sand mixture.

3.2. Swelling Heave and Cumulative Infiltration

The cumulative water infiltration was obtained from the integral of the volumetric water content profiles. The soil heave was determined from the soil surface level at different times measured by the X ray attenuation contrast at the border between soil and water (Figures 3a and 3b). For the bentonite-sand mix (Figure 3a), during the first 10 min, both cumulative infiltration and soil heave increased linearly with squared root of time followed by a slower increase. Soil heave, as expected, was less than the amount of infiltrated water.

For the vertisol (Figure 3b) both cumulative infiltration and soil heave increased more gradually than that for the bentonite-sand mixture. At the end of the experiment, water continued infiltrating whereas swelling rate decreased.

3.3. Kinetics of Swelling

Both materials were divided into three layers. The top two layers were, initially, 1 cm each. The initial height of the third layer was 1.6 cm for the bentonite-sand mix and 4.1 cm for the vertisol. The layer thicknesses changed with time because of the soil swelling. Each layer contained the same amount of dry material during the experiment. The contribution of each layer to the total rise of the soil (Figures 4a and 4b) was calculated from the dry bulk density profiles.

For the bentonite-sand mix (Figure 4a), swelling was impor-

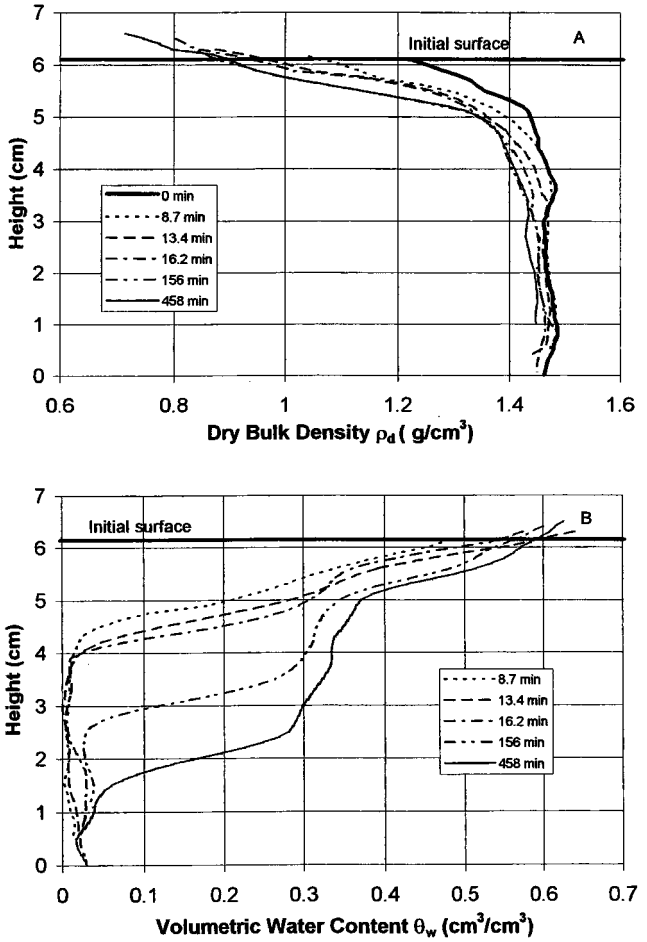

Figure 2. Observed profiles of (a) dry bulk density and (b) volumetric water content in the vertisol.

tant primarily during the first 15 min. The contribution of the initial first top layer to the total rise was 43%. The second and third layers contributed to 36 and 21%, respectively.

For the vertisol (Figure 4b) the soil swelled 0.4 cm during the first 100 min and 0.2 cm thereafter. The first centimeter of the soil contributed to 80% of the total rise. The two remaining layers contributed only 10% each.

In both cases, the swelling was greater in the beginning of the infiltration and occurred mostly by the expansion of the first layer. In the vertisol the swelling process was slower than that in the bentonite-sand mix.

3.4. Hydraulic Properties

3.4.1. The swelling curve. Swelling curves (Figures 5a and 5b) were obtained with (4a) and (4b) from the experimental measurements. Each curve, obtained at different elevations, covers a different water content interval, but combination of all the swelling curves allows us to determine a global swelling characteristic. In both materials the swelling curves show two parts, called residual and normal domains in the direction of higher water contents [*Giraldez et al.*, 1983]. In the residual domain the change of the void ratio is smaller than the change of the moisture ratio. In the normal domain the change of the void ratio is equal to the change of the moisture ratio. In both materials the normal domain is a little higher than the saturated line, especially for the vertisol. This noticeable discrepancy could indicate the presence of some empty pores where the water could not enter and that characterizes the unsaturated swelling. For the bentonite-sand mix this discrepancy is not significant for the high moisture ratios. Both materials have very similar swelling characteristics in spite of different water content and dry bulk density profiles.

3.4.2. The diffusivity curve. Hydraulic diffusivities of water relative to the solid particles were calculated for both materials according to (8) from the experimental content profiles (Figures 6a and 6b). The hydraulic diffusivity curves versus moisture ratio were different at successive times. At a given moisture ratio the hydraulic diffusivity decreased with time.

For the mixture of sand and bentonite the curves were translated by less than two log cycles between the beginning of the experiment and 19 min and by one log cycle between 19 min and the end of the experiment (193.5 min). Therefore it seems that the decrease of diffusivity with time is important at the beginning of the experiment and less important at the end.

For the vertisol the hydraulic diffusivity of the first top centimeter of the column behaved differently than the rest, which is caused by the difference of the initial bulk density and by a bigger diffusion of the clay particles in contact with the water.

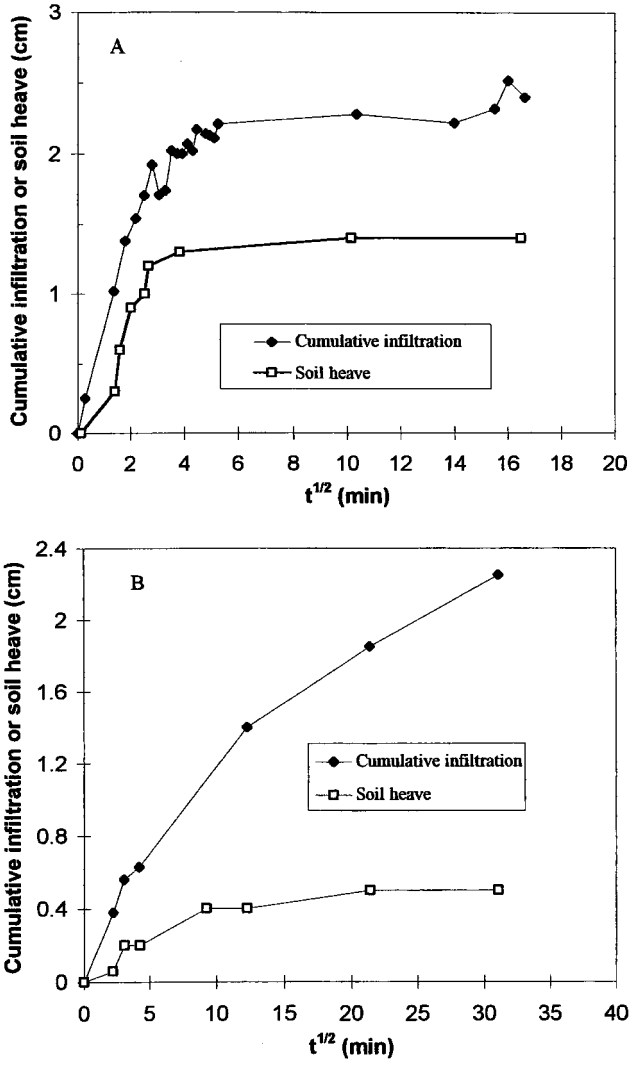

Figure 3. Swelling heave and cumulative infiltration for (a) the bentonite-sand mixture and (b) the vertisol.

The hydraulic diffusivity curves corresponding to the low moisture ratio (from 0.1 to 0.6 $cm^3\ cm^{-3}$) increased sharply (Figure 6a). The other part of the curve, from 0.6 to 1.5 or 2 $cm^3\ cm^{-3}$ of moisture ratio, was nearly constant and corresponds to the first centimeters of the soil, which swelled more than the deeper layers.

The observed decrease of the hydraulic diffusivity with time was more important for the bentonite-sand mixture than for the vertisol. The values of diffusivities obtained at the beginning of the infiltration experiments in both materials were from 1 to 0.1 $cm^2\ min^{-1}$. The hydraulic diffusivity was from 10^{-2} to $10^{-5}\ cm^2\ min^{-1}$ for bentonite after 193.5 min and around 10^{-2}–$10^{-3}\ cm^2\ min^{-1}$ for the vertisol after 458 min.

The decrease in the hydraulic diffusivity was caused by a decrease in pore space and connectivity due to aggregate swelling. At the beginning the water moved in the pores between the aggregates. Little by little, the water diffused into the aggregates, which then swelled, and progressively the volume of the interaggregate pores decreased. *Guerrini and Swartzendruber* [1992] also observed a similar phenomenon on some types of dry nonswelling soils that they attributed to a microlevel rearrangement of soil aggregates.

The high initial hydraulic diffusivity observed in Figure 6 is related to the very rapid expansion of the first centimeter of the soil observed in Figure 4. The decrease of diffusivity that followed is consecutive to a slower swelling of the soil. This phenomenon is in good agreement with the study of *Favre et al.* [1997], who observed, in a field, a very fast closure of the cracks immediately after the rain event followed by a decrease of the water infiltration.

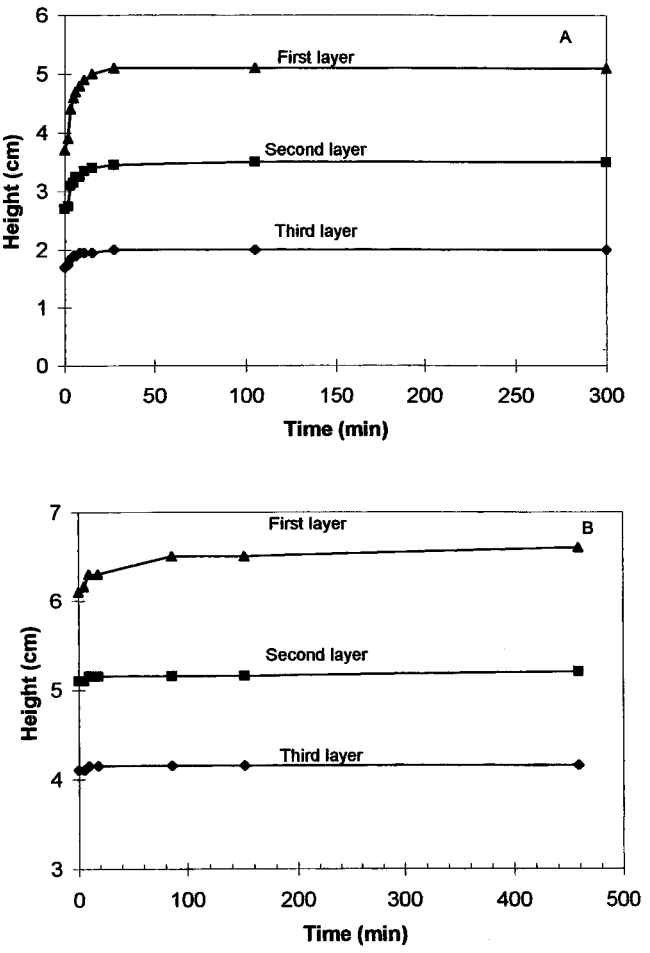

Figure 4. Height of the sample versus time and contribution of the different layers for (a) the bentonite-sand mixture and (b) the vertisol.

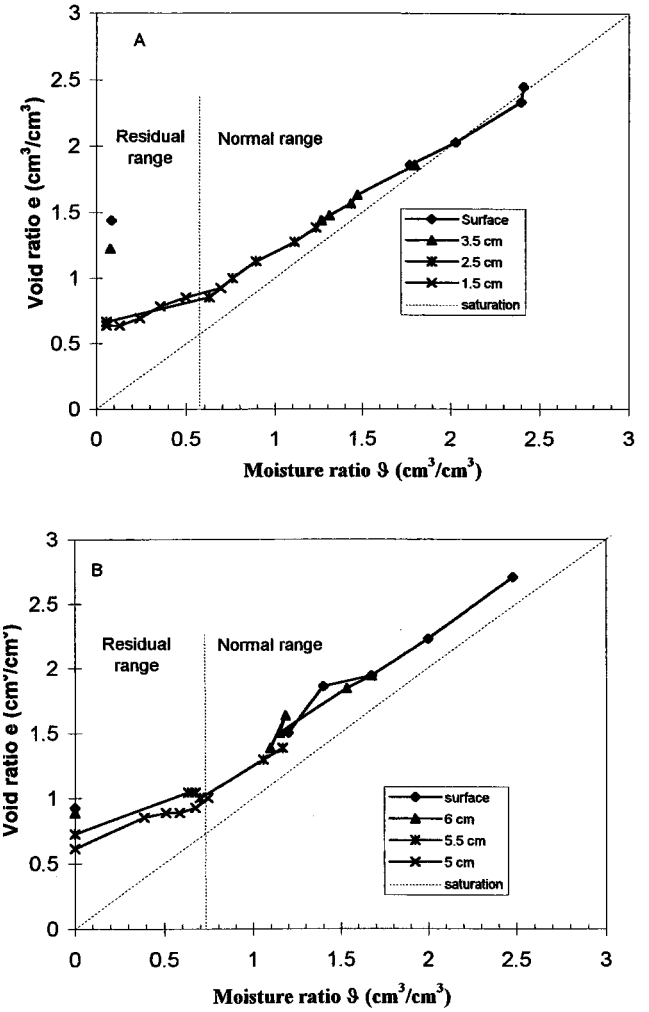

Figure 5. Experimental swelling characteristics of (a) a bentonite-sand mixture and (b) a vertisol at different heights in the samples.

4. Conclusion

Apparently for the first time, a dual-energy synchrotron X ray technique was used to monitor water content and bulk density changes in swelling soils. Because of their high intensity and brightness, synchrotron X rays should, in principle, allow measurements in swelling systems, even during the very fast, initial phase of the swelling, immediately after the onset of infiltration. Experimental results obtained with a bentonite-sand mix and with a vertisol confirm the potential of the dual-energy X ray technique. These results demonstrate that the swelling rate is very high at the beginning of infiltration experiments and that it decreases markedly afterwards. These observations are in general agreement with the well-documented rapid closure of cracks in desiccated vertisols when they are moistened (e.g., during a rainfall event). This swelling pattern, with an initially fast kinetics followed by an appreciably slower

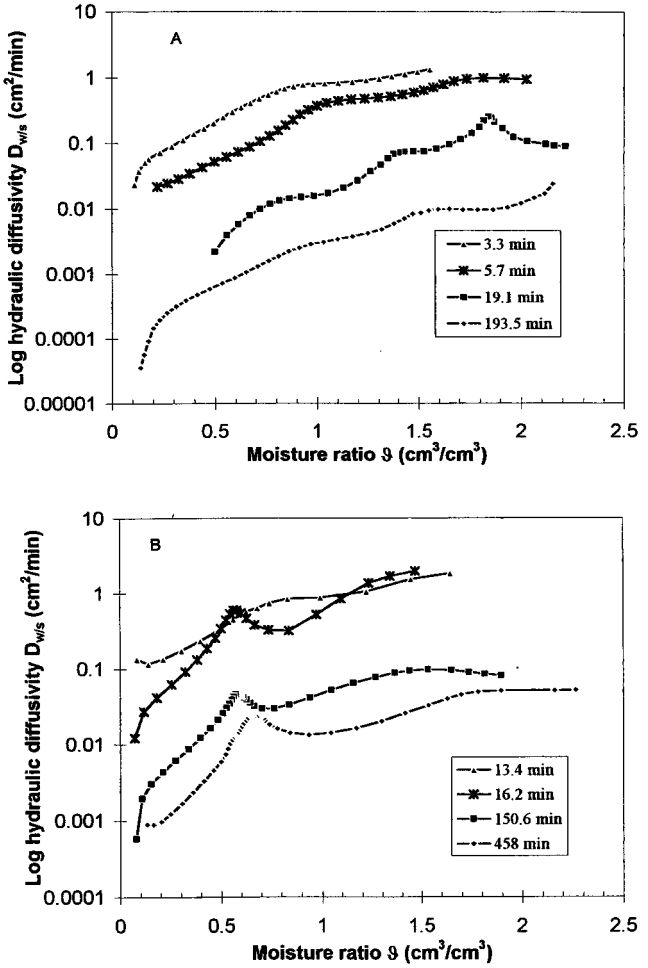

Figure 6. Hydraulic diffusivity of (a) the bentonite-sand mixture and (b) the vertisol, versus moisture ratio at different times during the infiltration experiments.

one, may be linked with the evolution of the hydraulic diffusivity of the soil. Hydraulic diffusivity decreases sharply, by several orders of magnitude, immediately after water application, which could be due to aggregate swelling and the resulting changes on the pore size.

Acknowledgment. We would like to thank the staff of the Cornell High Energy Synchrotron Source for their technical support.

References

Angulo-Jaramillo, R., Caractérisation hydrodynamique de sols déformables partiellement saturés: Etude expérimentale à l'aide de la spectrométrie gamma double source, Ph.D. dissertation, 210 pp., Inst. Natl. Polytech. de Grenoble, France, 1989.

Barataud, F., D. Stemmelen, and C. Moyne, Identification of the hydraulic diffusivity of a soil by inverse method with dual-energy gamma ray attenuation measurements, in *Parameter Identification and Inverse Problems in Hydrology, Geology and Ecology*, edited by J. Gottlieb and P. DuChateau, pp. 123–132, Kluwer Acad., Norwell, Mass., 1996.

Batterman, B. W., and N. W. Ashcroft, CHESS: The new synchrotron radiation facility at Cornell, *Science*, *206*, 157–161, 1979.

Charlie, W. A., D. Durnford, and T. S. Steenhuis, Rapid density profiling of consolidating clay using synchrotron radiation, *Geotech. Test. J.*, *20*(5), 340–346, 1997.

DiCarlo, D. A., T. W. J. Bauters, T. S. Steenhuis, J.-Y. Parlange, and B. R. Bierck, High-speed measurements of three-phase flow using synchrotron X rays, *Water Resour. Res.*, *33*, 569–576, 1997.

Favre, F., P. Boivin, and M. C. S. Wopereis, Water movement and soil swelling in a dry, cracked vertisol toposequence, *Geoderma*, *78*, 113–123, 1997.

Garnier, P., E. Perrier, R. Angulo-Jaramillo, and P. Baveye, Numerical model of 3-dimensional anisotropic deformation and dimensional water flow in swelling soils, *Soil Sci.*, *162*(6), 410–420, 1997a.

Garnier, P., M. Rieu, P. Boivin, M. Vauclin, and P. Baveye, Determining the hydraulic properties of a swelling soil from a transient evaporation experiment, *Soil Sci. Soc. Am. J.*, *61*, 1555–1563, 1997b.

Gérard-Marchant, P., R. Angulo-Jaramillo, R. Haverkamp, M. Vauclin, P. Groenevelt, and D. E. Elrick, Estimating the hydraulic conductivity of slowly permeable and swelling materials from single-ring experiments, *Water Resour. Res.*, *33*, 1375–1382, 1997.

Giraldez, J. V., G. Sposito, and D. Delgado, A general soil volume change equation, *Soil Sci. Soc. Am. J.*, *47*, 419–422, 1983.

Guerrini, I. A., and D. Swartzendruber, Soil water diffusivity as explicitly dependent on both time and water content, *Soil Sci. Soc. Am. J.*, *56*, 335–340, 1992.

Liu, Y., B. R. Bierck, J. S. Selker, T. S. Steenhuis, and J.-Y. Parlange, High intensity X-ray and tensiometer measurements in rapidly changing preferential flow fields, *Soil Sci. Soc. Am. J.*, *57*, 1188–1192, 1993.

Nofziger, D. L., and D. Swartzendruber, Material content of binary physical mixtures as measured with dual-energy beam of gamma rays, *J. Appl. Phys.*, *45*, 5443–5449, 1974.

Oostrom, M., J. H. Dane, B. C. Missildine, and R. J. Lenhard, Error analysis of dual-energy gamma radiation measurements, *Soil Sci.*, *160*(1), 28–42, 1995.

Philip, J. R., Hydrostatics and hydrodynamics in swelling soils, *Water Resour. Res.*, *5*, 1070–1077, 1969.

Smiles, D. E., and M. J. Rosenthal, The movement of water in swelling materials, *Aust. J. Soil Res.*, *6*, 237–248, 1968.

Talsma, T., and A. van der Lelij, Infiltration and water movement in an in situ swelling soil during prolonged ponding, *Aust. J. Soil Res.*, *14*, 337–349, 1976.

Vachaud, G., D. Dancette, S. Sonko, and J.-L. Thony, Méthodes de caractérisation hydrodynamique in situ d'un sol non saturé: Application à deux types de sol du Sénégal en vue de la détermination des termes du bilan hydrique, *Ann. Agron.*, *29*(1), 1–36, 1978.

Watson, K. K., An instantaneous profile method for determining the hydraulic conductivity of unsaturated porous materials, *Water Resour. Res.*, *2*, 709–715, 1966.

R. Angulo-Jaramillo, Laboratoire d'étude des Transferts en Hydrologie et Environnement, VMR 5564 CNRS, INPG, ORSTOM, VJF, LTHE, B.P. 53, 38041 Grenoble cedex 9, France.

T. W. J. Bauters, C. J. G. Darnault, P. Garnier, J.-Y. Parlange, and T. S. Steenhuis, Department of Agricultural and Biological Engineering, Cornell University, Riley-Robb Hall, Ithaca, NY 14853. (e-mail: tssl@cornell.edu)

P. Baveye, Laboratory of Environmental Geophysics, Cornell University, Bradfield Hall, Ithaca, NY 14853.

D. A. DiCarlo, Department of Petroleum Engineering, Stanford University, Stanford, CA 94305.

(Received December 23, 1997; revised July 6, 1998;
accepted July 14, 1998.)